Silicon (2018) 10:967–974
DOI 10.1007/s12633-017-9554-9

ORIGINAL PAPER

Synthesis and Characterization of SnO_2 on Porous Silicon for Photoconversion

Falah A-H Mutlak[1] · Ahmed B. Taha[1] · Uday Muhsin Nayef[2]

Received: 18 October 2016 / Accepted: 25 January 2017 / Published online: 27 June 2017

Abstract A photoconversion device was fabricated based on SnO_2 film prepared by a chemical spray pyrolysis technique. The SnO_2 nanofilms were grown on the porous silicon (PS) nanosurface. Various affecting parameters were studied such as different current densities 20, 30, 40, 50 and 60 mA/cm^2 with 16% HF concentration for 10 min at a substrate temperature of 400 °C. The structural, morphological and detector properties were measured. X-ray diffraction (XRD) confirmed the formation of porous silicon and the crystal size was reduced toward the nanometric scale of the face centered cubic structure, while the diffraction peaks of other SnO_2 peaks were found to be much weaker compared to standard SnO_2NPs. The Atomic Force Microscope (AFM) investigation showed the sponge-like structure of PS, the width of surface pits and surface roughness increased to a specific value then decreased with etching current density. This could be attributed to the different filling process depending on the pore sizes and homogenous distribution of PS. From the found photodetector measurements, the spectral responsivity and quantum efficiency curves included two regions; the first region was due to the absorption of UV light by SnO_2NPs. The second region corresponded to the visible light absorption with the PS layer and strongly depended on fabrication conditions.

Keywords Porous silicon · SnO_2 films · Spray pyrolysis · Photodetectors

✉ Uday Muhsin Nayef
unayef@yahoo.com

Falah A-H Mutlak
falah.mutlak5@gmail.com

Ahmed B. Taha
hamody_basim@yahoo.com

[1] Department of Physics, College of Science, University of Baghdad, Baghdad, Iraq

[2] Department of Applied Science, University of Technology, Baghdad, Iraq

1 Introduction

Heterostructures formed by PS and transparent conductive oxides (TCO), such as SnO_2, have been of great interest in recent years. The interest lies in a wide range of properties of these junctions such as light emission [1], the realization of electrical contacts in the volume of the porous film improving the electroluminescence efficiency [2], and implementation of structures with particular sensing properties [3]. The aggregates used in these oxides tend to act as a dopant. Typical dopants in the case of SnO_2 may be F, Cl, or Sb. The inclusion of these dopants in SnO_2 alters the original oxide properties [4], not only those related to the electronic transport, but also modifying the structural properties like the lattice parameter. Many authors have discussed the influence of the doping level on crystalline silicon (c-Si) which is an important material of the last century that has been the cornerstone of the semiconductor industry and has spearheaded extraordinary technological advancement [5].

Bulk c-Si, however, has an indirect band gap, making it unsuitable for integrating light with electronics (optoelectronics). Thus, c-Si has only very poor luminescence in the near infrared 1100 nm region [6] consequently; there have been great efforts in the last decade to produce controlled light emission from silicon in the near infrared and visible regions [7]. The Porous Silicon (PS) high efficiency can be

obtained by using nanostructure silicon with different physical characteristics compared to the bulk structure including wide energy gap, and low reflective index compared to c-Si. The synthesis of SnO_2 can be done by a variety of methods, among them are: chemical vapor deposition [8], reactive sputtering [9], and spray pyrolysis [10]. These techniques allow the growth of materials in the form of thin films with a high degree of homogeneity [11].

In the present work, preparation and characterization of deposited SnO_2NPs by the spray pyrolysis method on PS photodetectors were demonstrated.

2 Experimental Work

The SnO_2 nanofilms were prepared by the chemical spray pyrolysis technique. These films were deposited on a PS layer heated to 400 °C. A 0.1 M spray solution was prepared by dissolving stannic chloride ($SnCL_4.5H_2O$) of 97.5% purity in 100 ml distilled water. The above solution was placed in the flask of an atomizer and spread by controllable pressurized nitrogen gas flow on the heated substrates. The spraying time was 5 sec, which was controlled by an adjustable solenoid valve. The heated substrate was left for 55 sec after each spraying run to give time for the deposited SnO_2 layer to dry. The optimum experimental conditions for obtaining homogeneous SnO_2 thin film at 400 °C were determined by the spraying time, the drying time and the flushing gas pressure. The schematic diagram of the CSP homemade system is shown in Fig. 1a.

PS samples were prepared from a n-type silicon wafer of resistivity 0.015 Ωcm and (111) orientation in photo-electrochemical system with the assistance of laser illumination. A composition of HF (48%) and ethanol in a ratio 1:2 was used for the electrolyte and the anodization was carried out with a constant time of 10 min. The samples of (1×1 cm^2) dimensions were cut from the wafer and rinsed with ethanol to remove dirt. In order to remove the native oxide layer on the samples, after cleaning the samples, they were immersed in HF acid in a Teflon beaker. The cell was made out of Teflon that is resistant against attack from the hydrofluoric acid electrolyte. The silicon wafer served as the anode and it was sandwiched between the top and the bottom parts of the Teflon. The cathode was a circular gold piece that was submerged in the hydrofluoric acid electrolyte, the cathode was held in place by the top part of the Teflon cell and an aluminum ring, see Fig. 1b.

X-ray diffraction (XRD-6000 Shimadzu) was used to investigate the structural properties of SnO_2NPs on PS and the surface morphology of the samples such as particle shape and size were identified by using atomic force microscopy (AFM) (SPM-AA3000). AFM is successfully associated with the three-dimensional topographical analysis of surfaces with high resolution (lower than atomic resolution) and roughness measurements at a scan area of 700×700 nm.

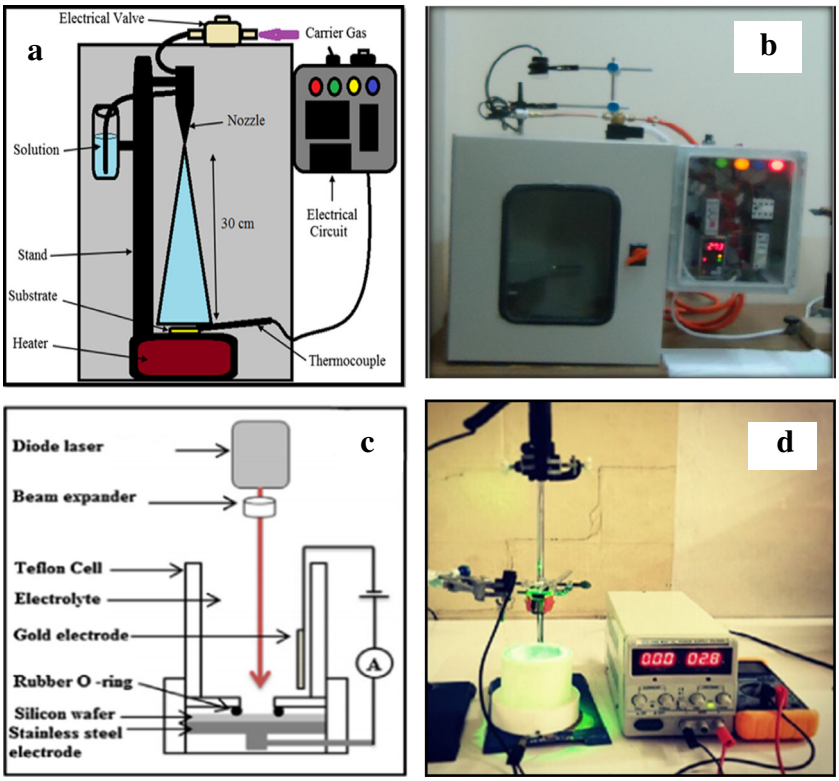

Fig. 1 (**a**) Schematic diagram of spray pyrolysis system, (**b**) photograph of spray pyrolysis setup, (**c**) Schematic drawing of the photo-electrochemical etching (PECE) and (**d**) photograph of PECE setup

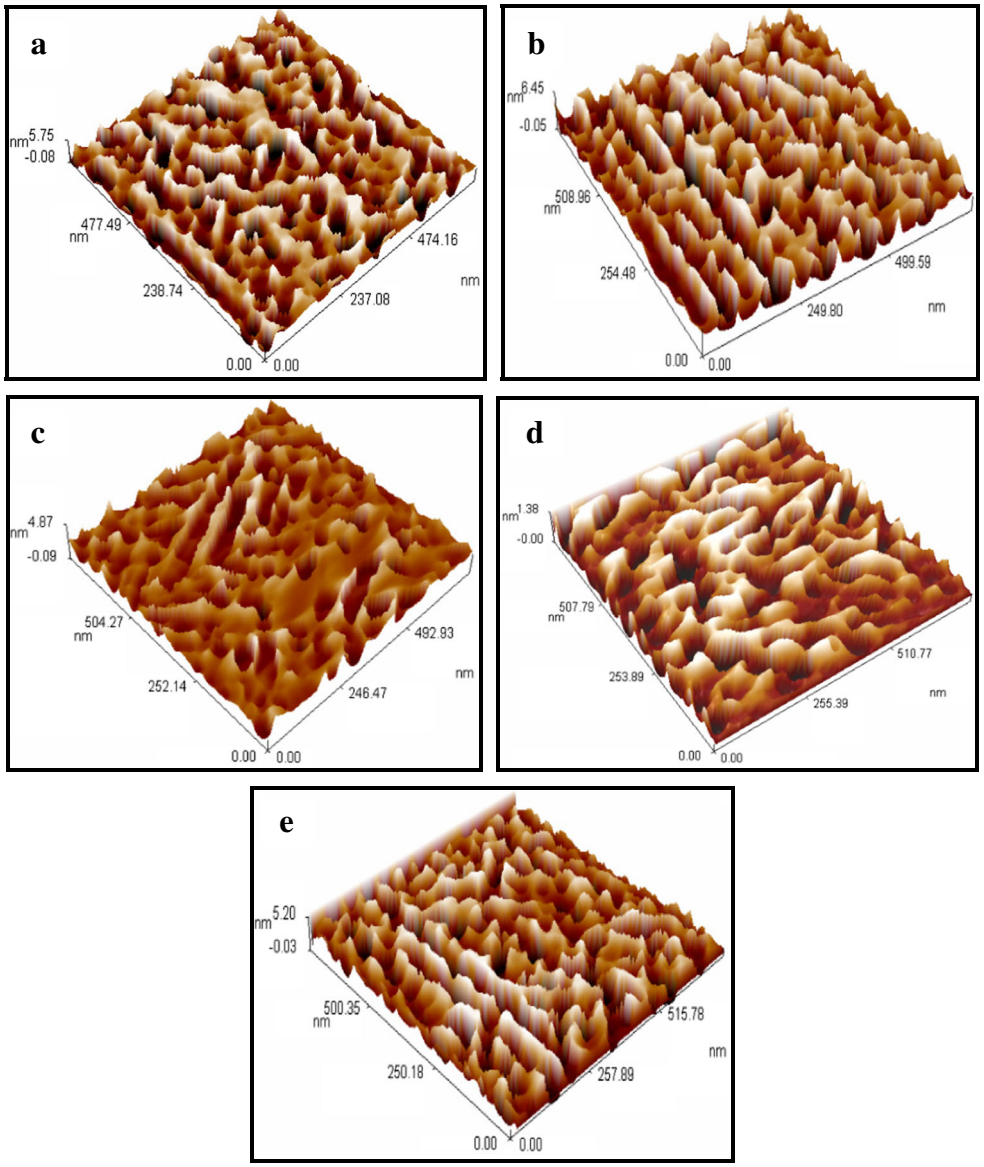

Fig. 2 3D AFM image of PS/SnO_2 NPs with etching current densities (**a**) 20, (**b**) 30, (**c**) 40, (**d**) 50 and (**e**) 60 mA/cm^2 in time 10 min

The light emitting devices were constructed in a sandwich structure, where the bottom and up electrode is aluminum (Al). The intermediate layer is composed of $SnO_2/PS/Si$.

The spectral responsivity (R_λ) of photodetectors was measured using a calibrated monochromator in the spectral region of (400–800 nm). The responsivity (R_λ) was determined by using (1)

$$R_\lambda = \frac{I_p}{\phi_p} \tag{1}$$

Where is the measured photocurrent and is the incident optical power.

The quantum efficiency (the conversion efficiency of photons to electrons) of the detector for a given wavelength,

$$\eta = \frac{hv}{q} R_\lambda \tag{2}$$

Where h is Planck's constant, v is the frequency of the optical signal and q is the electron charge. This expression is also given in terms of λ, the wavelength of the optical signal, and has units of amperes per watt (A/W).

Table 1 The calculated morphology characteristics of SnO_2/PS prepared with different current densities

Time of etching (min.)	Current density (mA/cm^2)	Average diameter (nm)	Average roughness (nm)
10	20	47.40	1.460
	30	52.01	1.590
	40	53.20	0.613
	50	55.89	0.340
	60	44.36	1.240

A more useful figure of merit is the specific detectivity (D^*) by using (3), which does not depend on the bandwidth and detector active area (S_{det}), Δf is the frequency response ($1/2\pi\tau$) and *NEP* is the noise equivalent power [12].

$$D^* = \frac{\sqrt{S_{det}}\Delta f}{NEP} \tag{3}$$

Through the absorption of electromagnetic radiation it is possible to identify the bandwidth detection, peak responsivity, peak detectivity and the amplitude of the photocurrent generated by a detector [13]. For a high-performance photodetector five requirements should be satisfied including high sensitivity, high signal-to-noise ratio, high spectral selectivity, high speed, and high stability [14].

3 Results and Discussion

3.1 The Surface Morphology of SnO_2 NPs/PS

The surface morphology of synthesized SnO_2NPs/PS was investigated by using AFM. The surface morphology properties of the SnO_2NPs/PS prepared by photoelectrochemical etching for porous and chemical spray pyrolysis technique for SnO_2 have been studied. The surface morphology of SnO_2NPs/PS was confirmed by AFM as shown in Fig. 2. The SnO_2NPs were prepared at 400 °C by spray pyrolysis and deposited on PS etched at 20, 30, 40, 50, and 60 mA/cm^2 current densities with 16% HF concentration for 10 min. As shown in Fig. 2, the SnO_2NPs are partially filling or completely covering pores. This is due to the surface of the PS layer which has a sponge-like structure consisting of a large number of pores with high surface area that make PS an adhesive surface for accommodating SnO_2NPs into its pores. Thus, the SnO_2NPs acted as a transparent capping and provided a good coverage of the PS surface, which could improve the structural stability of the PS substrate. From Table 1 the pore diameter increases to a specific value and then decreases. For lower currents, the chance for the hole to reach the surface is small due to the typical electrical field distribution at surface irregularities hence enough F^- ions are present at the interface, therefore, pore growth occurs in the silicon substrate. But for larger currents, the diffusion of the F^- ions reaching to the interface is slower than holes transport leading to the saturation state of the top surface of the silicon atoms with holes, and every ion that migrates there is met with a

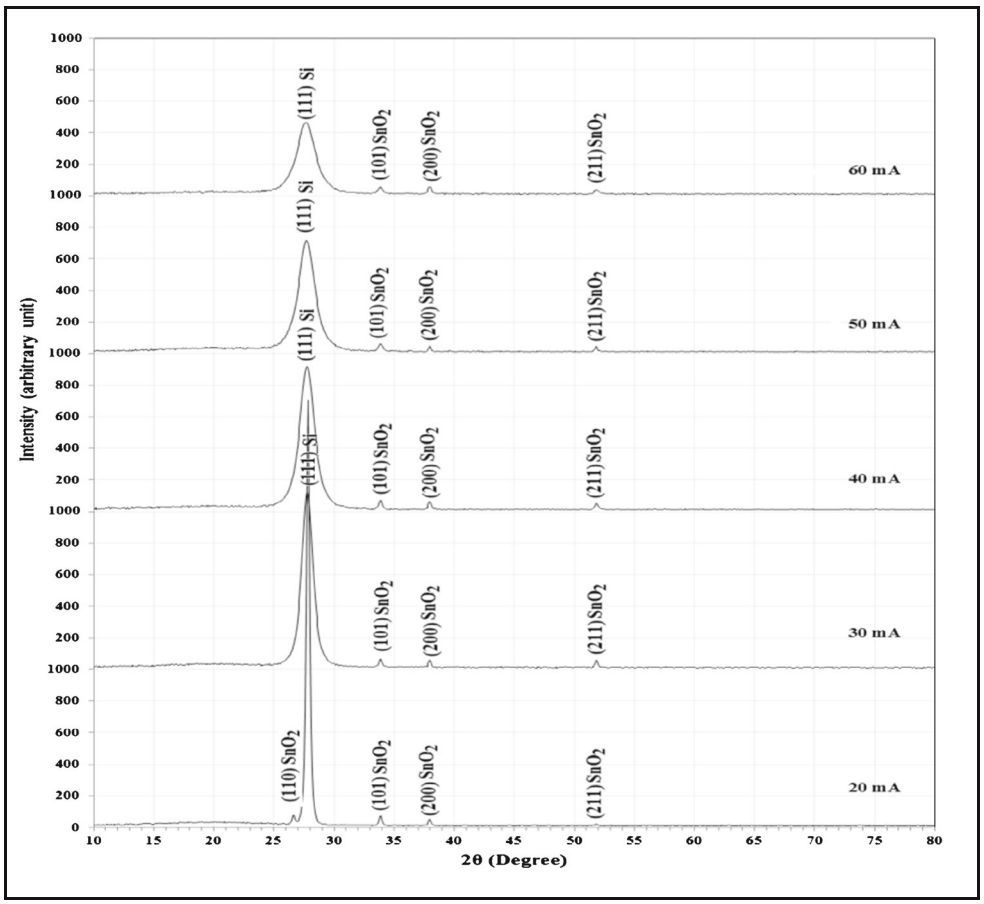

Fig. 3 shows the typical XRD patterns of deposited SnO_2NPs/PS at different current densities 20, 30, 40, 50, and 60 mA/cm^2, and constant etching time 10 min, temperature of substrate 400 °C

hole to dissolve silicon. As current passes, large amounts of the silicon structure are removed; this behavior is called the electro-polishing process [12]. However, due to etching time, the process would be repeated with a new polished layer until another pore is formed with specific size diameter as the time stops. Furthermore, the average roughness is changed according to the size of the pore diameter. These observations are in good agreement with the reported results [15].

The porous layer consists of many voids that propagate in the direction perpendicular to the surface. As shown in Table 1, the average diameter and roughness of SnO_2NPs deposited on PS increase with increasing current densities then decrease. This can be attributed to the different filling process depending on the pore sizes and homogenous distribution of PS. This shows how the structure growth depends on the PS morphology. The increasing in roughness represents a very important parameter to enhance the photoconversion process for optoelectronics devices [16].

3.2 Structural Characteristics of SnO_2NPs/PS

The X-ray diffraction (XRD) pattern of the SnO_2 nanofilm deposited on a nanospike layer of n-type silicon substrate is illustrated in Fig. 3.

The XRD pattern reveals three peaks at etching current 30, 40, 50, and 60 mA/cm^2 and four peaks for SnO_2 at 20 mA/cm^2. At (101), (200), and (211) they are for etching current 30, 40, 50, and 60 mA/cm^2 and planes for etching current 20 mA/cm^2 (110), (101), (200), and (211). Where at the plane (111) for Si a peak becomes broad with varying (FWHM) for the PS sample, the mismatch between Si and PS is clear because in PS the X-ray diffraction is from nano-sized crystals in the walls between pores. Consequently, we can confirm that the PS layer remains crystalline, but it is slightly shifted to a smaller diffraction angle. This result is attributed to the effect of strain which leads to an expanded lattice parameter and then the PS peak is displaced to a small

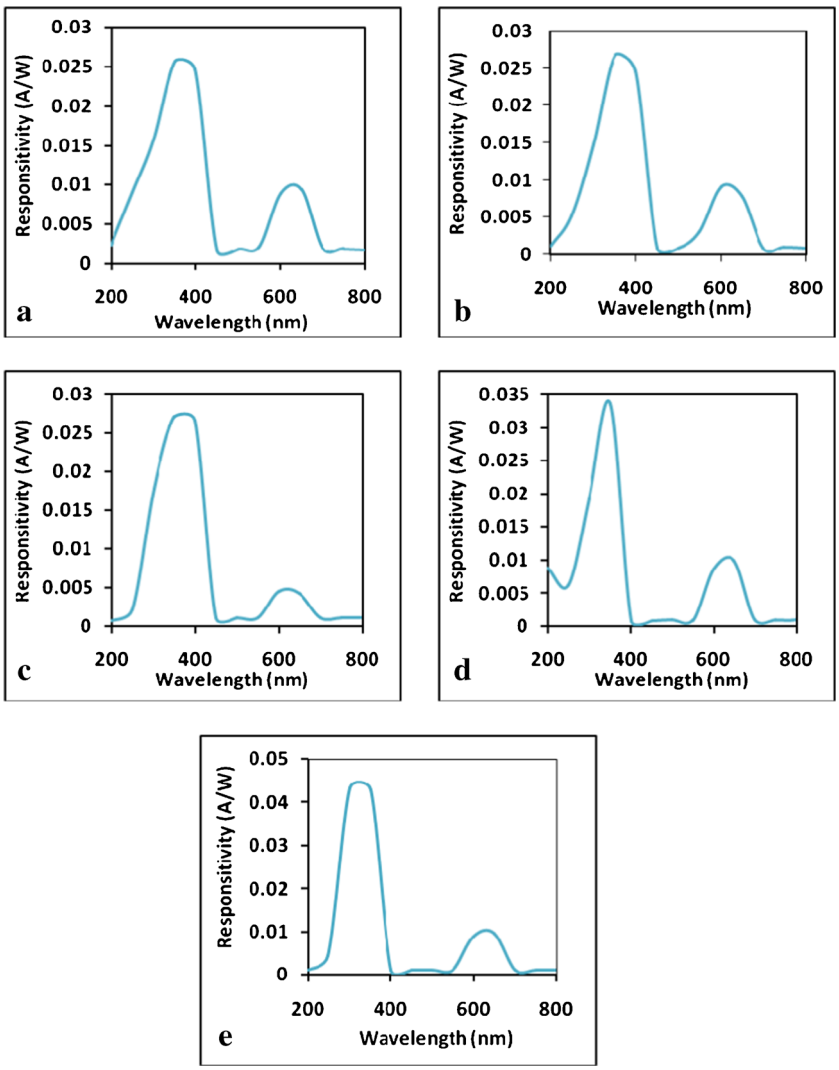

Fig. 4 Responsivity of SnO_2NPs/PS/n-Si samples prepared at 400 °C on PS at different current density (**a**) 20, (**b**) 30, (**c**) 40, (**d**) 50, and (**e**) 60 mA/cm^2 with 16% HF concentration for 10 min

diffraction angle and when crystalline size of PS decreases than the bulk Si peak. In addition, when the SnO_2 is sprayed on PS, a very thin layer of SnO_2 is formed above the PS structure after filling the inner walls of the pores as well. To ascertain the incorporation of the SnO_2 into the pores, from Fig. 3, it is noticed that the peak becomes broader with increasing the current density. This confirms the formation of pores on the silicon, and the SnO_2 makes the peak of the junction sharper than porous because of the SnO_2 filling the inner walls of the pores. These observations are in good agreement with the mentioned results [17].

3.3 Photodetector of SnO_2NPs/PS Measurements

The spectral responsivity (R_λ) is an important parameter to determine the spectral performance range of a photodetector. Figure 4 shows the responsivity as a function of wavelength for Al/SnO_2NPs/PS/n-Si/Al samples fabricated from SnO_2NPs prepared at 400 °C by spray pyrolysis and deposited on PS etched at 20, 30, 40, 50, and 60 mA/cm^2 current density with 16% HF concentration for 10 min.

The spectral responsivity curve includes two regions; the first region illustrates higher responsivity due to the absorption of the UV region in the range of 240–410 nm by SnO_2NPs. The second region corresponds to the visible light absorption in the range of 590–720 nm with the PS layer. After that, the reduction in the responsivity is observed which is attributed to the absorption of light by the silicon substrate. The prepared sample at current density 20 mA/cm^2 showed lower responsivity reaching to 0.025 A/W compared with 0.043 A/W for that prepared at a current density of 60 mA/cm^2. The enhancement results come from the good matching in structures between SnO_2 and PS then higher energy can be absorbed by the PS. In addition, as the PS structure changes in size, the responsitivity varies as with the pore size change. Also the responsivity curve is shifted toward the visible region due to reduction in the energy gap.

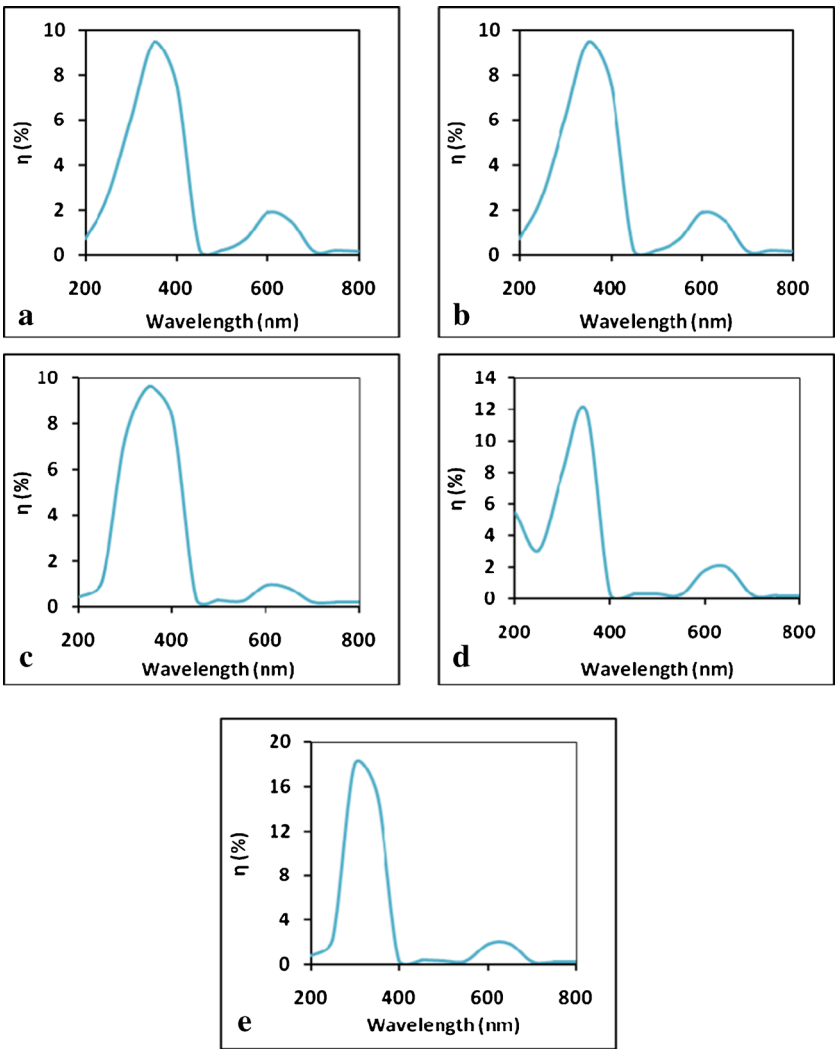

Fig. 5 Quantum efficiency of SnO_2NPs/PS samples prepared at 400 °C deposited on PS at different current density (**a**) 20, (**b**) 30, (**c**) 40, (**d**) 50, and (**e**) 60 mA/cm^2 with 16% HF concentration for 10 min

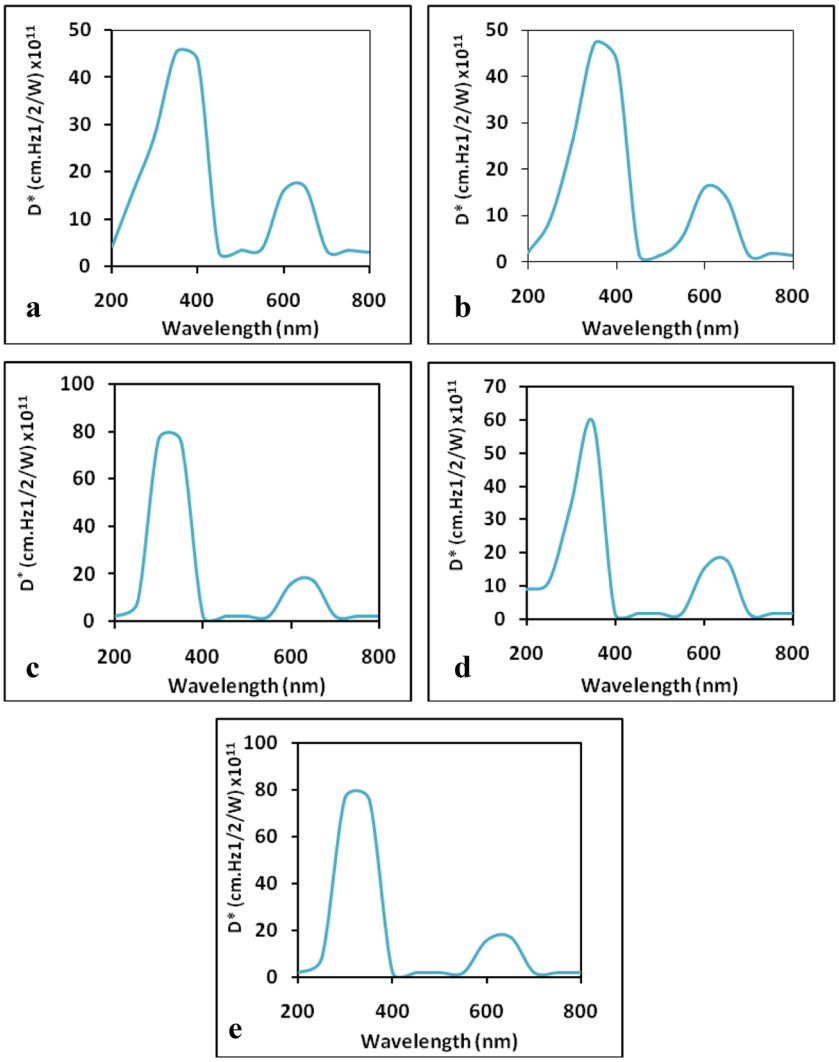

Fig. 6 Detectivity of SnO_2NPs/PS/n-Si samples prepared at 400 °C and deposited on PS at different current density (**a**) 20, (**b**) 30, (**c**) 40, (**d**) 50, and (**e**) 60 mA/cm^2 with 16% HF concentration for 10 min

Figure 5 illustrates the quantum efficiency (η) of Al/SnO_2NPs/PS/n-Si/Al samples prepared at 400 °C by spray pyrolysis and deposited on PS etched at 20, 30, 40, 50, and 60 mA/cm^2 current densities with 16% HF concentration for 10 min. As the etching current density is increased, the band-gap of the structure increases and hence the quantum efficiency becomes high, as the quantum efficiency is directly related to the spectral responsivity. The value of quantum efficiency is increased from 9.12% to 18% with increasing of etching current density from 20 mA/cm^2 to 60 mA/cm^2.

Moreover, the detectivity (D*) was also measured and it was found that samples have high values (see Fig. 6). The dark current was very small which indicated a lower noise to signal ratio leading to better detection because of the low dark current of SnO_2/PS with increasing of etching current of PS. These observations are in good agreement with the reported results [18].

4 Conclusions

In this work, the SnO_2 films were deposited on chemically etched n-type silicon substrate. The reduction in SnO_2NPs size accompanied by increasing the surface area to volume ratio and photoreaction of these nanoparticles led to increases of the responsivity, quantum efficiency and detectivity of this UV region detector.

References

1. Daoudi K, Sandu CS, Moadhen A, Ghica C, Canut B, Teodorescu VS, Blanchin MG, Roger JA, Oueslati M, Bessaïs B (2003) Mater Sci Eng B 101:262
2. Macedo AG, de Vaconcelos EA, Valaski R, Muchenski F, da Silva Jr. E. F., da Silva AF, Roman LS (2008) Thin Solid Films 517:870
3. Comini E, Faglia G, Sberveglieri G (2001) Sens: Actuators, B 76:270

4. Esteves MC, Gouvêa D., Sumodjo PTA (2004) Appl Surf Sci 229:24
5. Patwardhan SV, Clarson SJ (2012) Biological and bioactive silicon systems. Silicon 4:1–3
6. Prabakaran R, Kesavamoorthy R, Singtt A (2005) Mate Sci 28:219
7. Teo EJ, Mark BH, Bettiol AA, Karasi DM, Chameaux F, Watt F, Blackwood DJ (2006) Breese Adv Nater 18: 51
8. Calestani D, Zha M, Zappettini A, Lazzarini L, Salviati G (2005) Mater Sci Eng C 25:625
9. Muto Y, Oka N, Tsukamoto N, Iwabuchi Y, Kotsubo H, Shigesato Y (2011) Thin Solid Films 520:1178
10. Elangovan E, Singh MP, Ramamurthi K (2004) Mater Sci Eng B 113:143
11. Moadhen A, Elhouichet H, Romdhane S, Oueslati M, Roger JA, Bouchriha H (2003) Semicond Sci Technol 18:703
12. Ramizy A, Hassan Z, Omar K (2011) J Mater Sci: Mater Electron 22:717–723
13. Faria LA, Nohra LFM, Gomes NAS, Alves FDP (2012) Int J Optoelectron Eng 2(3):12–17
14. Chan S (2000) Porous silicon multilayer structure, thesis. University of Rochester, Rochester, p 155
15. Nayef UM, Muayad MW, Khalaf HA (2014) Eur Phys J Appl Phys 66:20104
16. Liao M, Sang L, Teraji T, Imura M, Alvarez J, Koide Y (2012) Japan J Appl Phys 51:7
17. Vidhya VS, Murali KR, Subramanian B, Manisankar P, Sanjeeviraja C, Jayachandran M (2011) J Alloys Compd 509(6):2842–2845
18. Nayef UM (2017) Optik 130:441–447